SEMARAK ILMU PUBLISHING

Journal of Advanced Research in Applied Sciences and Engineering Technology

Journal homepage:
https://semarakilmu.com.my/journals/index.php/applied_sciences_eng_tech/index
ISSN: 2462-1943

Effect of Ground Motion on Fragility and Vulnerability of Reinforced Concrete Bridge in Different Soil Conditions

Elwin Yu You Kuan[1], Nordila Ahmad[1,*], Siti Khadijah Che Osmi[1], Jestin Jelani[1], Thamer Ahmad Mohammad[2]

[1] Department of Civil Engineering, Faculty of Engineering, National Defence University of Malaysia, Sungai Besi Camp, 57000 Kuala Lumpur, Malaysia
[2] Department of Water Resources Engineering, College of Engineering, University of Baghdad, Baghdad Governorate, Iraq

ARTICLE INFO

Article history:
Received 3 January 2024
Received in revised form 20 May 2024
Accepted 25 June 2024
Available online 31 July 2024

Keywords:

Fragility curves; earthquake; seismic intensity; infrastructure resilience; RC bridges; vulnerability assessment

ABSTRACT

Bridges are essential components of transportation networks, serving as lifelines for the movement of people and goods. The bridges' resilience to natural disasters, particularly earthquakes, is an issue of paramount significance. Yet, a critical knowledge gap exists when it comes to understanding how bridges perform in the challenging terrain of medium-density sandy and clay soils during seismic events. This study seeks to bridge that gap by developing fragility curves that quantitatively evaluate the likelihood of bridge damage or failure across varying levels of earthquake magnitudes. The CSI Bridge v25.0.0 was used to simulate earthquake ground motions specifically within medium-density sandy and stiff clayey soils. Nonlinear time history analyses of the bridge were performed by using 5 different earthquake events with PGA ranging from 0.25 – 1.5g. Fragility analysis is performed to develop seismic fragility curves for the critical part of the bridge for various peak ground acceleration (PGA) in two types of soil conditions. The findings revealed that the deck component is more susceptible to damage than the pier. The impact of seismic activity on medium-dense soil is more significant than on stiff clayey soils in relation to the critical components of the bridge. This result enhances the ability to design bridges that can withstand and recover from seismic events more effectively.

1. Introduction

Transport infrastructure, particularly bridges, is significantly vulnerable to natural hazards, including earthquakes. The occurrence of The Great East Japan Earthquake in 2011, resulted in the documentation of significant structural damages to 300 bridges. This evidence highlights the susceptibility of bridges to earthquake disasters. Indonesia ranks second among the countries most exposed to natural disasters in the world. This is mainly due to the country's unique geographical characteristics, being surrounded by volcanic plateaus, making the country susceptible to earthquakes [1]. Earthquakes (EQ) in Peninsular Malaysia are mostly caused by tectonic activity in

* *Corresponding author.*
E-mail address: nordila@upnm.edu.my

https://doi.org/10.37934/araset.49.2.118133

Sumatra. With reference to Syuib *et al.,* [2], a series of severe earthquakes, such as the 2004 Sumatra Earthquake, the 2005 Nias Earthquake, and the 2007 Bengkulu Earthquake, have reactivated the long-dormant fault system in Peninsular Malaysia. According to Silva *et al.,* [3], earthquakes are responsible for an average of 20,000 deaths per year worldwide. Malaysia cannot prevent calamities like those detected in the region [4] where Malaysia lies on the relatively stable Sunda Plate and the semi-stable South China Sea region, exposing the country to seismic activity from Sulawesi and the Philippines, especially Sabah and Sarawak [5]. A case study was conducted by Rosli *et al.,* [6] on the Mesilau River basin due to the earthquake and rainfall caused by the 2015 Sabah earthquake. Agricultural land and MRN bridges were destroyed [7]. Overall, Malaysia faces low to moderate seismic hazard, with seismic sources originating from regional and local movements. Bridge performance during earthquakes is an important aspect of infrastructure resilience and public safety. Bridges are particularly vulnerable to earthquake damage due to their vulnerable location and exposure to many natural hazards [8]. Figure 1 shows bridges that collapsed due to seismic activity. The 2011 Tohoku-Oki earthquake, with a magnitude of 9.0, occurred on March 11, 2011, causing significant damage over a wide area. This damage included the washing away of the main bridge girders, as shown in Figure 1(a), due to the combination of seismic motion and subsequent tsunami [9]. The under-construction Yadanatheinkha Bridge in Figure 1(b) collapsed after the Thabeikkyin earthquake in Myanmar on November 11, 2012 [10]. Baihwa Bridge, a continuous-span reinforced concrete structure, collapsed at the rotating part due to the earthquake, as shown in Figure 1(c). This can be due to weak connections, insufficient reinforcement, small stirrups, and insufficient bearing strength [11]. On September 21, 1999, a powerful earthquake struck Chi-Chi, Taiwan, with a magnitude of 7.6 on the moment magnitude scale. This seismic event resulted in significant deformation of the Earth's crust in the central Taiwan region. The earthquake resulted in an 85-km-long surface rupture along the Chelungpu fault [12] while pier wall of the Wu-Shi Bridge failed due to shear stress caused by the Chi-Chi earthquake as shown in Figure 1(d). Thus, from all these damages, it gives strong evidence that the bridges become vulnerable to natural hazards especially to earthquake disasters.

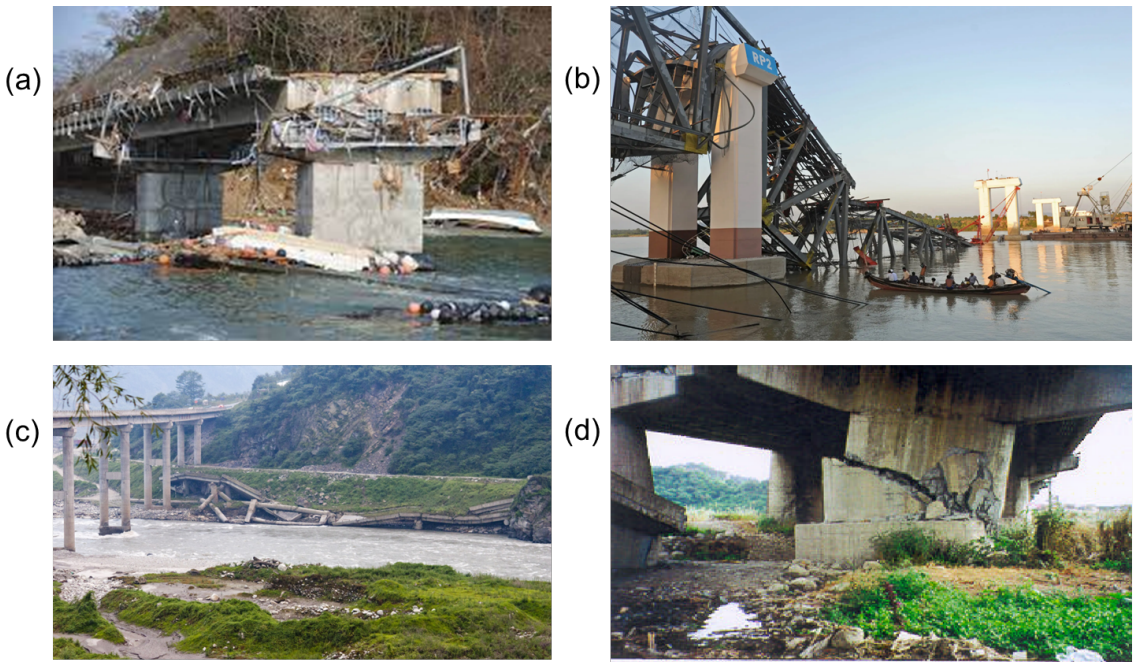

Fig. 1. Bridges damage in various countries (a) Tohoku-Oki earthquake, Japan in 2011 (b) Thabeikkyin earthquake, Myanmar in 2012 (c) Wenchuan earthquake, China in 2008 (d) Chi-Chi earthquake, Taiwan in 1999

Seismic fragility analysis has grown in importance as a method of assessing the seismic response of bridge structures as more bridges had experienced major earthquakes event which causes the loss in economic and fatalities. The current emphasis in the analysis of fragility curves is focused on three distinct categories, namely analytical fragility curves, empirical fragility curves, and fragility curves derived from expert opinions [13]. The aforementioned curves offer a quantitative assessment of the potential harm and assist in the evaluation of the seismic hazard linked to bridge structures [14]. It is used to assess the seismic performance of bridge structures situated in different soil conditions sandy when subjected to earthquakes [15,16]. Nevertheless, there is still a dearth of empirical data regarding bridge damage caused by ground motion and the development of analytical fragility curves specifically tailored to the seismic performance of bridges situated in medium density sandy soil and stiff clayey soils. Prior studies have highlighted those bridges located on sandy and clay soils are particularly susceptible to seismic damage due to the amplification of ground motion and the occurrence of soil liquefaction phenomena [17]. Besides, the correlation between the bridge structure and the underlying soil is a pivotal element in seismic performance. The integration of this interaction into the understanding of fragility poses a significant challenge and thus data gathering for numerical analysis of bridge performance under seismic hazard is deemed vital. Therefore, this study employs dynamic nonlinear time history analysis to examine the seismic vulnerability of a reinforced concrete (RC) bridge subjected to various dynamic analyses based on the data from past earthquakes events with various moment magnitude (M_w).

The objective of this study is to develop fragility curves by quantitatively assess the likelihood of bridge failure or collapse based on a series of thorough dynamic analyses of the bridge. The analyses were performed using a finite element modelling (FEM).

2. Methodology

2.1 Numerical Model of the Bridge

The bridge being assessed in this context is a prestressed concrete structure featuring three spans, collectively measuring 100.5 meters in length with reference to the paper from Argyroudis *et al.,* [18]. Its components are constructed using C30/37 concrete, characterized by a unit weight of γ=25 kN/m^3 and an elastic modulus of E=3.3 x 10^7 kN/m^2. The Poisson ratio utilized is 0.2. The reinforcement applied in building the bridge model includes rebar with a unit weight of γ=76.97 kN/m^3 and an elastic modulus of E=1.999 x 10^8 kN/m^2. The structural steel incorporated in the construction is of grade S355, with a unit weight of γ=76.97 kN/m^3 and an elastic modulus of E=2.1 x 10^8 kN/m^2. The bridge's tendon, featuring a unit weight of γ=76.97 kN/m^3 and an elastic modulus of E=1.965 x 10^8 kN/m^2, spans three equal-length segments, each measuring 33.5 meters. The bridge is supported by two piers and two integral abutments extending to full height, as illustrated in Figure 2.

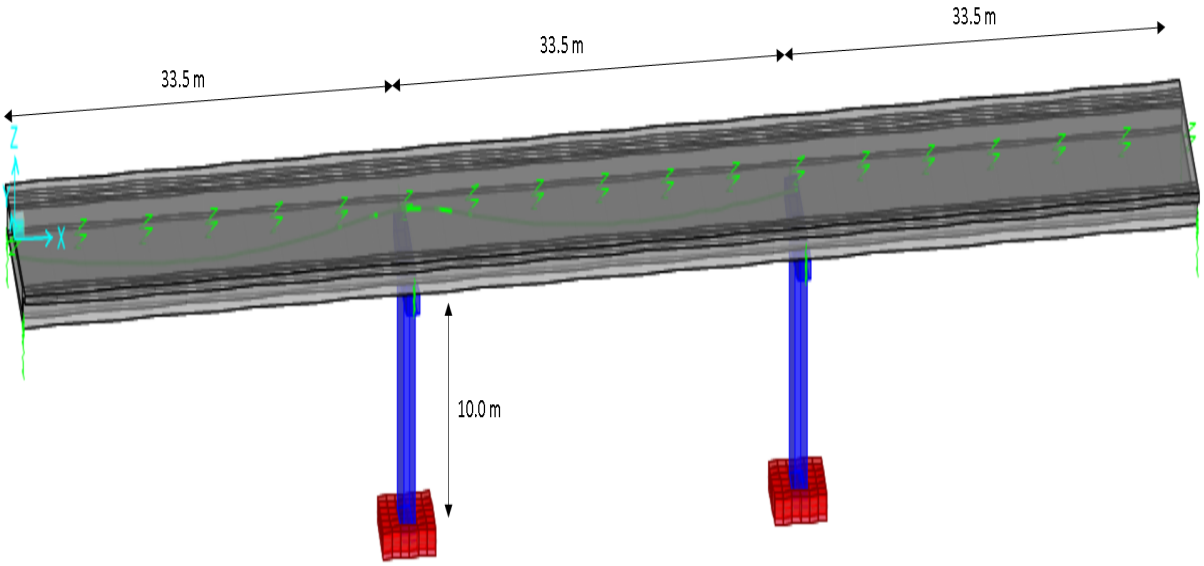

Fig. 2. Finite element of a reinforced concrete (RC) bridge

The bridge deck is designed as a box girder, with a total width of 13.5 meters and a total depth of 1.5 meters. The relevant information on the bridge section specifications for the concrete box girder of the deck can be found in Table 1 below.

Table 1
Dimension of the bridge section data for the concrete box girder

Slab and Girder Thickness	Units
Top Slab Thickness (t1)	0.305 m
Bottom Slab Thickness (t2)	0.205 m
Exterior Girder Thickness (t3)	0.600 m
Fillet Horizontal Dimension Data	Units
f1 Horizontal Dimension	0.46 m
f2 Horizontal Dimension	0.46 m
f3 Horizontal Dimension	0.15 m
f4 Horizontal Dimension	0.46 m
f5 Horizontal Dimension	0.46 m
f6 Horizontal Dimension	0.15 m
f7 Horizontal Dimension	0.46 m
f8 Horizontal Dimension	0.46 m
Fillet Vertical Dimension Data	Units
f1 – f8 Vertical Dimension	0.00 m
Left Overhang Data	Units
Left Overhang Length (L1)	0.915 m
Left Overhang Outer Thickness (t5)	0.350 m
Right Overhang Data	Units
Right Overhang Length (L2)	0.915 m
Right Overhang Outer Thickness (t6)	0.350 m

Figure 3 shows the bridge section data for the concrete girder box depicted from the FEM which was required in order to construct the bridge section and all the bridge and soil properties were entered into the FEM, CSI Bridge software and the data can be found in Table 1.

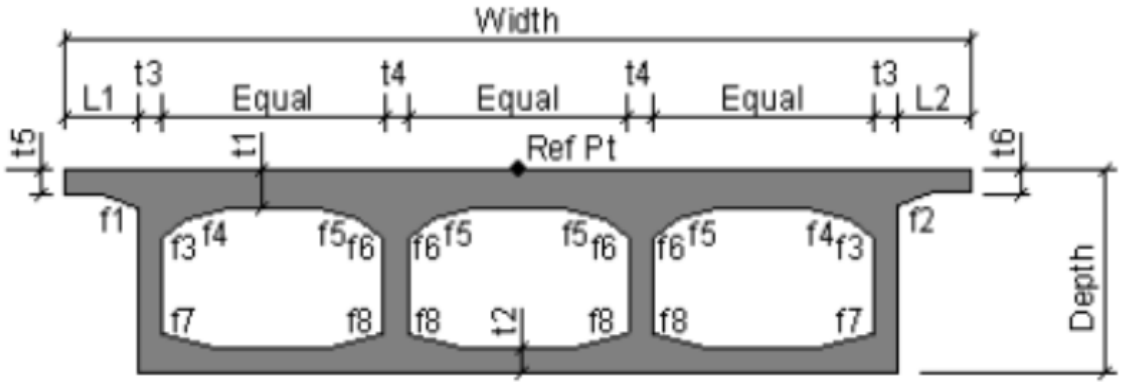

Fig. 3. The depicted concrete box girder bridge section of the deck

The abutments are connected to the girder bottom only and supported with fixed foundation spring. The piers are constructed as wall-type sections, with dimensions of 1 meter by 4.5 meters in the longitudinal and transverse directions, respectively, and they stand at a height of 10 meters. Additionally, the shallow foundation footing for the piers is one meter thick and measures 3.5 meters in both length and width.

As shown in Table 2, the soil stratum properties were also classified into two distinct soil types. The soil-foundation-structure interaction is dependent on their soil's shearing capacity, as stated by Lin *et al.,* [19]. The study assessed the soil-foundation interaction by employing the methodology outlined in FEMA 356 [20].

Table 2
Soil layer properties

Soil Type	Layer Thickness, m	Modulus of Subgrade Reaction (k_s), kN/m^3	Shear Factor
Medium Dense Sand	30	40000	0.1
Stiff Clayey soil	30	32000	0.1

The suggested model assumes that the shallow-bearing footings are inflexible and utilizes the uncoupled spring model depicted in Figure 4 to describe the underlying soil support.

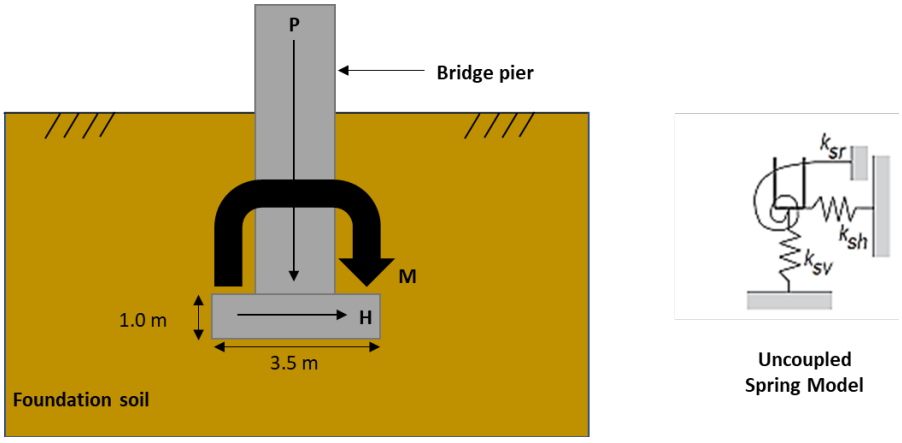

Fig. 4. Shallow foundation with uncoupled spring system

The bridge is subjected to a distributed load of 18.5 kN/m/m, by taking into consideration for both the self-weight of the deck and live loads, as specified in Eurocode 8-Part1. The bridge lane was also defined to identify where vehicle loads operate on the superstructure of a bridge. The two floating lanes were specified at a width of 3.6576 meters. The five actual time histories earthquakes

data recorded were downloaded from Pacific Earthquake Engineering Research Center (PEER) ground motion database. The earthquakes data used are Duzce (Duzce), Mw=7.14, Turkey, 1999; Kocaeli (Gebze), Mw=7.51, Turkey, 1999; Umbria Marche (Gubbio-Piana), Mw=5.7, Italy, 1997; Hector Mine (Hector), Mw=7.13, USA, 1999; Fruli (Barcis), Mw=6.5, Italy, 1976. In the dynamic analyses, the time histories are scaled so that their PGAs increases from 0.25 to 1.50 g with a step of 0.125 g. Various load cases for the nonlinear modal time history analyses had been introduced for earthquakes data scaled down to PGA ranging from 0.25 to 1.50 g. There will be a constant damping of 5% for all modes. In addition, the process of scaling PGA is beneficial for doing bias analysis, specifically for aftershock ground motions. Engineers can evaluate the influence of PGA scaling and detect any potential biases by comparing different intensity metrics. This research enhances the precision of scaling methods and enhances the accuracy of seismic design. The acceleration of all earthquake's events was plotted in Figure 5. In Figure 5 (a), (b), (c), (d) and (e) showed the data recorded by stations on the earthquake events that happened in Duzce station, Turkey in year 1999, Gebze station, Turkey in year 1999, Gubbio-Piana station, Italy in year 1997, Hector station, USA in year 1997 and Fruli station, Italy in year 1976.

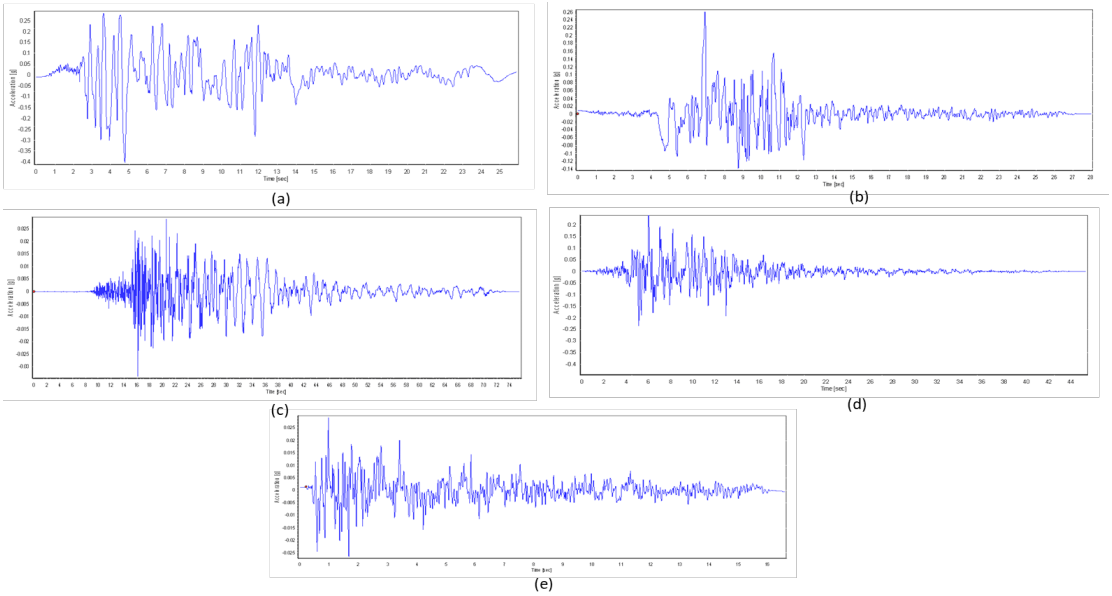

Fig. 5. Ground motion retrieved from PEER

To summarize, scaling the PGA up to 1.5 is a technique employed to capture the fundamental seismic properties required for constructing structures capable of withstanding seismic occurrences with an increased level of safety and dependability. Engineers can utilize this tool to generate precise design response spectra and do comprehensive ground motion analysis. The scale factor of each earthquakes event needs to be calculated based on the Eq. (1) [21] below to be inserted into the CSI Bridge for nonlinear dynamic time history analyses. Hence, a comprehensive examination was conducted on a total of 110 combinations pertaining to the bridge model. These combinations encompassed 2 distinct types of soil, 5 seismic inputs, and 11 levels of PGA.

$$Scale\ Factor, f = \frac{Target\ PGA}{Actual\ PGA} \quad (1)$$

When performing nonlinear dynamic analyses of bridges, it is essential to carefully select recorded ground motions that match the design spectrum of the region of interest [22]. The other seismic records were obtained from the PEER Ground Motion Database and were auto-generated to

match the seismic response spectrum of the bridge area. These records are considered international seismic records. In accordance with the recommendations of the EuroCode 8 National Annex, the accelerograms were selected to have a mean value that matches the seismic response spectrum of the bridge area, as shown in Figure 6.

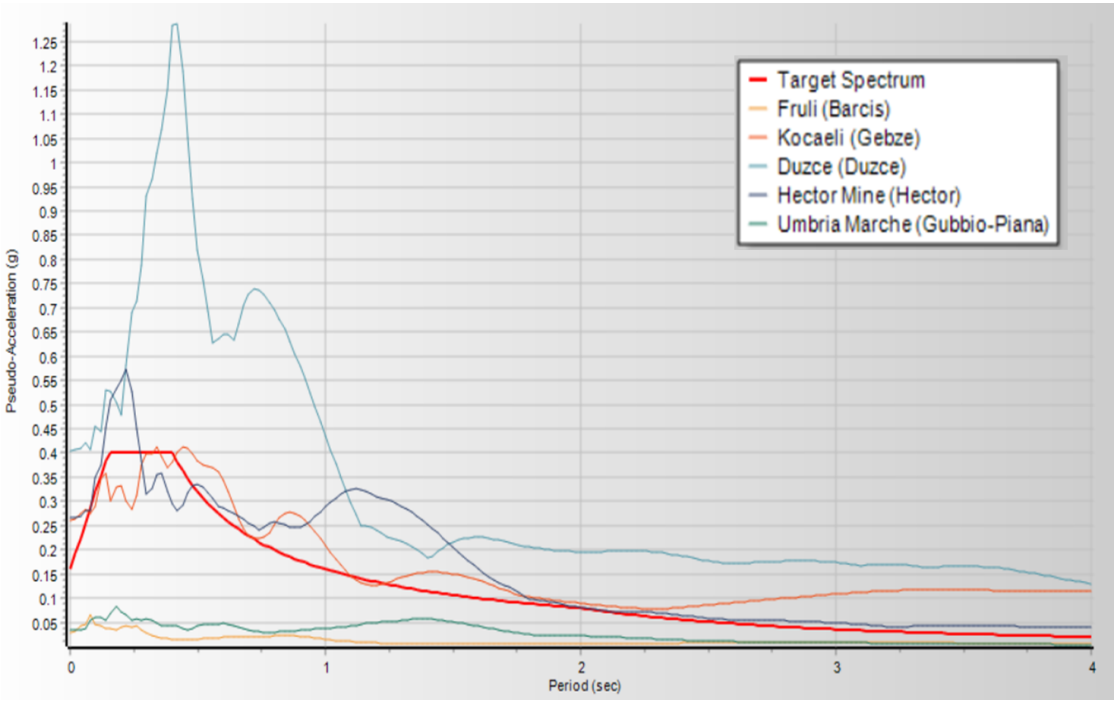

Fig. 6. The response spectrum is matched to the selected ground accelerations

2.2 Establishment of the Seismic Fragility Curves

Fragility functions are mathematical models that quantify the probability of surpassing certain limit states based on a specific earthquake intensity measure (IM), which in this case is defined as the PGA under bedrock settings. Fragility curves are commonly characterised by a lognormal probability distribution function as shown in Eq. (2) [23,24]. The development process involves the establishment of two parameters, namely IM_{mi} (which represents the median threshold value of IM required to induce the i^{th} damage state) and β_{tot} (representing the overall lognormal standard deviation).

$$P(DS \geq DSi|IM) = \Phi\left[\frac{In\left(\frac{IM}{IM_{mi}}\right)}{\beta_{tot}}\right] \quad (2)$$

The correlation of the IM, i.e., PGA for earthquakes, and the related engineering demand parameters (EDP) was used to generate fragility functions for each bridge component. The latter was calculated using the results of numerical simulations for the maximum bending moment (BM) along the deck and maximum vertical displacement of the pier, taking into consideration various seismic hazard actions and the uncertainty in the demand (B_D) based on two distinct types of soil, i.e., medium density sand and stiff clayey soil. A variety of estimated EDPs resulting from the modification of hazard intensities and their effects, i.e., ground movements for EQ. The appropriate threshold values in Table 3 had been defined by Argyroudis and Stergios [25], a best-fit regression was used to calculate the median threshold intensity measure (IM_{mi}) for each damage state for all bridge components [26]. The selection of the maximum bending moment (M_{max}) as the EDP for the essential

components of the deck is performed for the purpose to be used as a representative of structural failure. The calculation of the total variability (β_{tot}) incorporates three sources of uncertainty and is performed in accordance with Eq. (3), assuming statistical independence. Based on Yuan *et al.,* [27], uncertainty associated with the definition of damage states (β_{ds}) is preset to be 0.4, while the uncertainty attributable to capacity (β_C) is set at 0.3 based on opinion from experts. The standard deviation of the residuals of the computed EDP versus the best fit regression is used to assess the uncertainty in response to hazard actions (B_D).

$$\beta_{tot}{}^2 = \beta_C{}^2 + \beta_D{}^2 + \beta_{ds}{}^2 \quad (3)$$

The criteria for determining the minor damage state of the bridge deck are the occurrence of concrete cracking and steel yielding. The yielding bending moment (M_y) is indicative of the level of moderate damage sustained by the deck. Conversely, the thresholds for the substantial damage state of the deck are characterised by a bending moment of $1.5M_y$. The drift ratio is regarded as an alternative EDP for the pier, and Jain *et al.,* [28] have implemented the damage thresholds established by Kim and Shinozuka [29] in Table 3.

Table 3
Classification of bridge components through defining damage states

Component	Deck	Pier
EDP Damage States	BM	drift ratio (%)
Minor	M_{cr}	0.7
Moderate	M_y	1.5
Extensive	$1.5M_y$	2.5

3. Results

The numerical bridge model was constructed and by applying the dead load on the static bridge model. Since the bridge is asymmetrical, only 1 point on the top of the pier and third span of the deck will be selected as the EDP. Figure 7 shows the bending moment on the deck and displacement on pier from the static model. The point which shows the highest bending moment and maximum displacement were identified. Next, the time history analyses were simulated for 110 cases including 2 types of soil, 5 seismic inputs, and 11 levels of PGA.

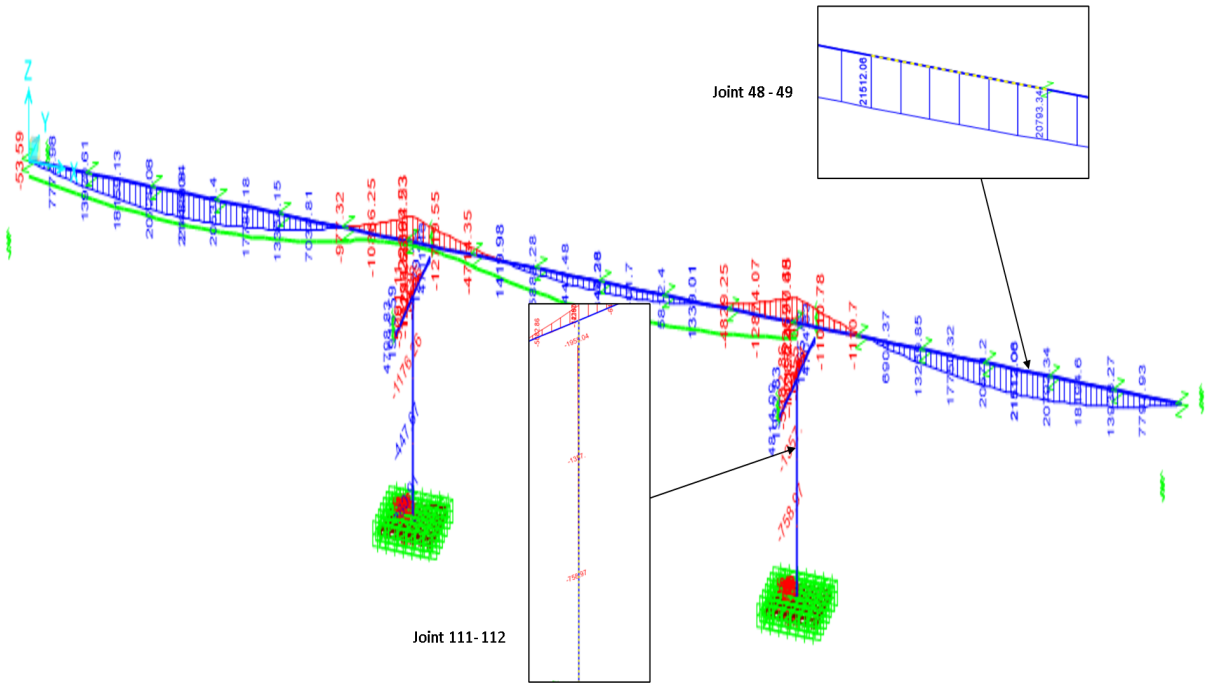

Fig. 7. Static RC bridge model under dead load condition

3.1 Derivation of Fragility Curves for Pier

A non-linear dynamic analysis is performed on the constructed models, whereby each model is subjected to a range of Peak Ground Accelerations (PGA) spanning from 0.25g to 1.5g. The link between the drift percentage and the applied ground motions for the selected pier with joint number 111-112 of the bridge model is shown by establishing the maximum drift percentage based on the maximum displacement of the pier. The damage state definitions for the bridge model are provided in Table 4.

Table 4
Defining the IM_{mi} for medium density sandy soil from the regression curve

Damage States	Drift (%) Limits	Damage Index (DI)	Ln DI	IM_{mi}
Minor	0.7	0.13	-2.04	0.55
Moderate	1.5	0.27	-1.31	1.11
Extensive	2.5	0.45	-0.80	1.97

The determination of the damage index for the piers was accomplished by Jain *et al.,* [28] using the utilisation of drift percentage limitations. The evolution of damage for pier drift ratio under various PGA at different type of soil were plotted. The natural logarithm of the IM_{mi} can be derived by determining the point of intersection between the best-fit line. The natural exponential function was utilised in the IM_{mi} to facilitate the computation of fragility curves. With reference to the regression curve the IM_{mi} for the medium dense sandy soil and stiff clayey soil are determined as in Table 4 and Table 5, respectively.

Table 5
Defining the IM_{mi} for stiff clayey soil from the regression curve

Damage States	Drift (%) Limits	Damage Index (DI)	Ln DI	IM_{mi}
Minor	0.7	0.13	-2.04	0.48
Moderate	1.5	0.27	-1.31	1.03
Extensive	2.5	0.45	-0.80	1.86

In Figure 8, an example from the paper by Argyroudis and Kaynia [30]. is presented where different data points signify the results of an analysis regarding the damage index across various levels of earthquake intensity. The solid line is the outcome of a regression analysis, and the median threshold value of the intensity measure (IM_{mi}) required to trigger the i^{th} damage state (ds_i) is calculated based on the definition of this damage state as determined by the damage index.

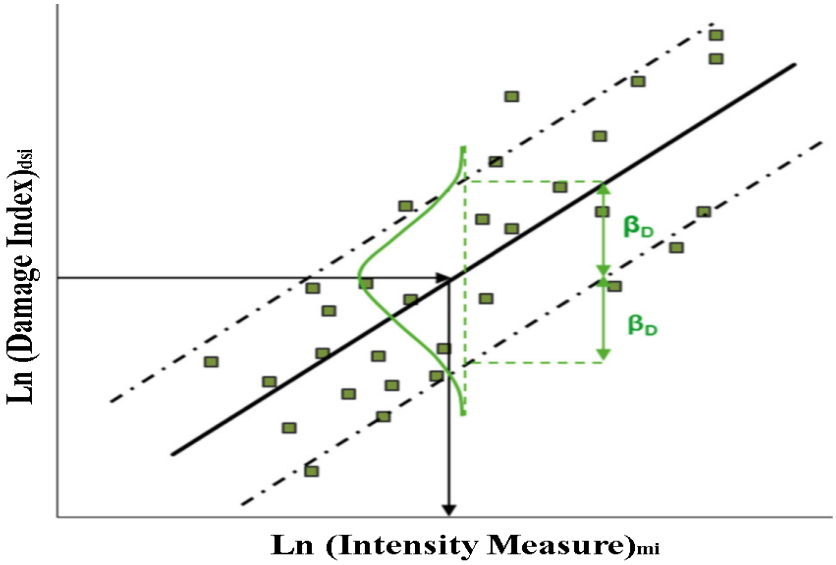

Fig. 8. Illustration of the damage evolves with the intensity measure (IM) of an earthquake, including the determination of the median threshold value (IM_{mi}) for a specific damage state (ds_i) and the standard deviation (β_D) influenced by the variability in input motion (demand)

Based on Eq. (3), it is one of the important parameters that is required for the derivation of fragility curves for the pier. The medium density sandy soil value for β_{tot} is calculated from Eq. (3), which is 0.87 where the value for β_D is equal to 0.71 by the dispersion in response due to the variability of the seismic input motion. The stiff clayey soil for the βtot value is calculated from Eq. (3), which is 0.71 and the value of β_D is 0.50. The derivation of the fragility curves in Figure 9, Figure 10 and Figure 11 is calculated based on the Eq. (2) which showed the comparison between the medium dense sandy soil and stiff clayey soil.

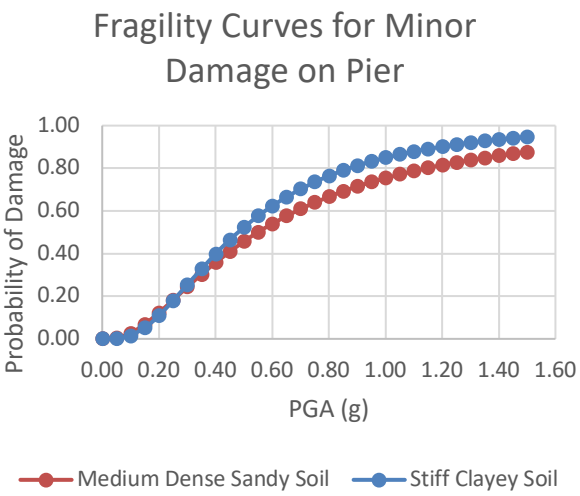

Fig. 9. Seismic fragility curves for minor damage on the RC bridge pier for different PGA levels

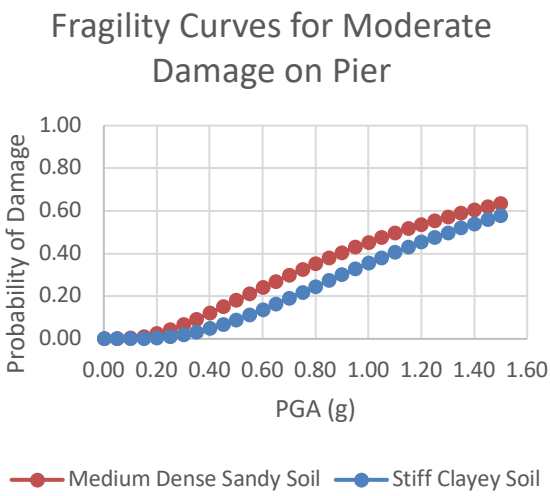

Fig. 10. Seismic fragility curves for moderate damage on the RC bridge pier for different PGA levels

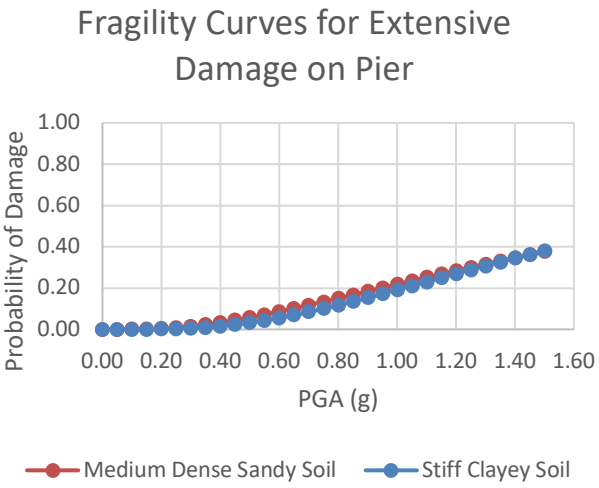

Fig. 11. Seismic fragility curves for extensive damage on the RC bridge pier for different PGA levels

Based on different IM_{mi} which was retrieved from Table 4 and Table 5, the probability of damage to happen on the pier is more significant on the medium density sandy soil foundation compare to the stiff clayey soil. The results of the fragility curves presented in Figure 9 indicate that for bridge piers, the probability of destruction under minor damage was approximately 76% in stiff clayey soil with a PGA of 0.8 g, as opposed to 67% in medium dense sandy soil. At medium-dense sandy soil, the probability that the pier will sustain damage decreases substantially at the same PGA of 0.8 g when subjected to moderate and extensive damage, from 35% to 15%, respectively. On the other hand, the stiff clayey soil also experiences the same decreasing probability from 25% to 12% in the fragility curves for moderate and extensive damage, as shown in Figure 10 and Figure 11. In the fragility curves for extensive damage on pier, the probability of the damage due to the effect of the medium density sandy soil and stiff clayey soil eventually will be almost equal as the seismic intensity increases to 1.5 g. To provide greater specificity, a bridge supported by a shallow foundation exhibits a more

resilient response characterized by the capacity to absorb energy. In scenarios where scouring is absent, there is a noted 20% increased susceptibility to "minor damage" in comparison to the two scouring scenarios examined [31]. Likewise, heightened vulnerability is observed across the spectrum of damage classes, including moderate, extensive, and complete damage. This observation is that the piers supported by shallow foundations dissipate a greater amount of energy, leading to increased hysteresis energy.

3.2 Derivation of Fragility Curves for Deck

The selection of the maximum bending moment (M_{max}) as the EDP for the crucial parts of the deck is made in order to accurately depict the potential structural collapse. Joint 48-49 is selected from the static model as shown in Figure 4 as it has the highest bending moment effect on the bridge. The criteria for designating the minor damage states of the bridge deck include the occurrence of concrete cracking and steel yielding (M_{cr}). The yielding bending moment (M_y) is the parameter that characterizes the level of moderate damage experienced by the deck. On the other hand, the thresholds indicating the extensive damage state of the deck are associated with a value of 1.5 times of the yielding bending moment ($1.5M_y$). The pertinent literature from the study by Tsionis and Fardis [32] through technical knowledge judgement, and the empirical equal displacement rule from Aydinoglu [33], the aforementioned assumptions are derived. The DI for the 3 different damage states is with reference to the derivation method by Argyroudis and Mitoulis [25]. The DI values for medium dense sandy soil and stiff clayey soil are presented in Table 6 and Table 7, respectively.

Table 6
Defining the IM_{mi} for medium dense sandy soil from the regression curve

Damage States	Damage Index (DI)	Ln DI	IM_{mi}
Minor	M_{cr}	4.71	0.05
Moderate	M_y	5.08	0.09
Extensive	$1.5M_y$	5.48	0.14

Table 7
Defining the IM_{mi} for stiff clayey soil from the regression curve

Damage States	Damage Index (DI)	Ln DI	IM_{mi}
Minor	M_{cr}	4.71	0.06
Moderate	M_y	5.08	0.10
Extensive	$1.5M_y$	5.48	0.14

The IM_{mi} can be obtained for each damage state using the regression curve from the evolution of damage with earthquake intensity with reference to Figure 8. Based on Eq. (3), the derivation of fragility curves for the deck is based on the maximum bending moment. The medium density sandy soil value for β_{tot} is calculated from Eq. (3), which is 0.62 and the value for β_D is obtained from the dispersion in response due to the variability of the seismic input motion which is 0.36. While for stiff clayey soil, the βtot value is calculated from Eq. (3), which is 0.60 and the value of β_D is 0.33. The derivation of the fragility curves in Figure 12, Figure 13 and Figure 14 is calculated based on the Eq. (2) which showed the comparison of the damage states between the medium density sandy soil and stiff clayey soil.

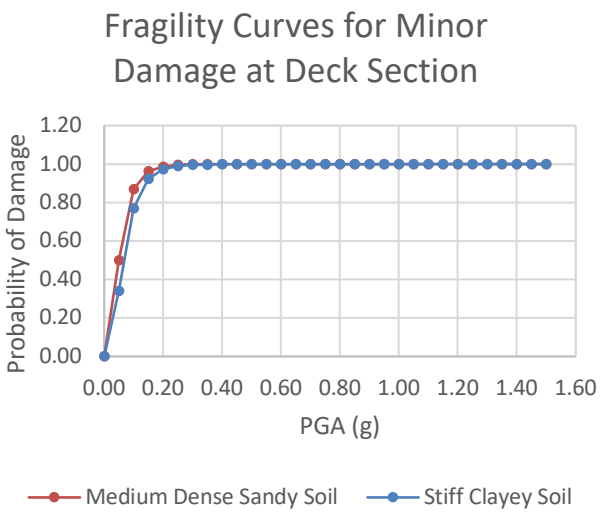

Fig. 12. Seismic fragility curves for minor damage on the RC bridge deck for different PGA levels

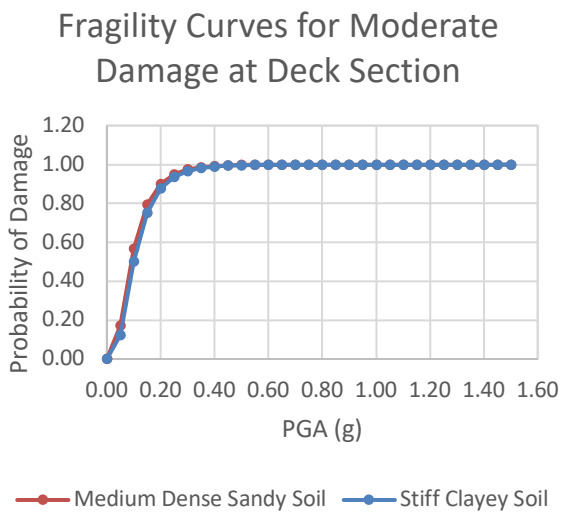

Fig. 13. Seismic fragility curves for moderate damage on the RC bridge deck for different PGA levels

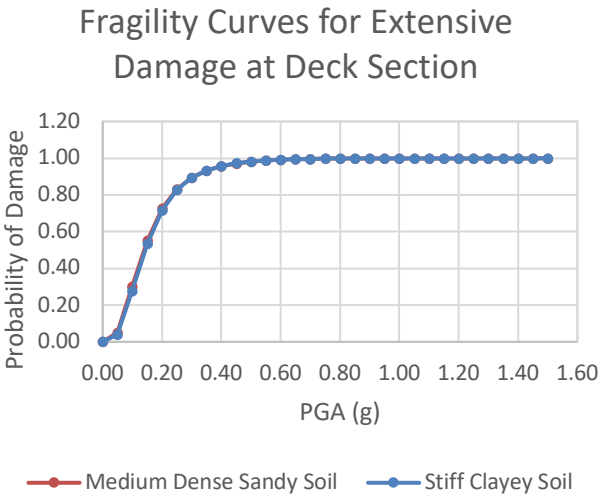

Fig. 14. Seismic fragility curves for extensive damage on the RC bridge deck for different PGA levels

Based on different IM_{mi} which was retrieved from Table 6 and Table 7, the probability of damage to happen on the deck is very significant at low PGA for both medium density sandy soil and stiff clayey soil. The results of the fragility curves presented in Figure 12 indicate that for bridge deck on Joint 48-49, the probability of destruction under minor damage was higher in medium dense sandy soil approximately 96% at PGA of 0.15 g, as opposed to 92% in stiff clayey soil. At medium-dense sandy soil, the probability that the deck to achieve 100% at minor, moderate and extensive damage are at 0.60 g, 1.05 g and 1.30 g. On the other hand, the stiff clayey soil also experiences the same increasing probability to 100 % at 0.70 g for minor damage, 1.05 g for moderate damage and 1.50 g for extensive damage. Hence, the bridge deck experiences the higher probability of damages as the deck cannot take the effect of the seismic intensity. The study results on bridge decks demonstrate a consistent damage pattern across various soil types for all damage classes. This suggests that the type of soil may not substantially influence the level of damage experienced by bridge decks during

seismic events. The consistent nature of these results indicates that elements such as the bridge decks' design, construction, materials, and structural structure may have a greater influence on the level of damage observed. The principal elements that influence the damage levels encountered by bridge decks during seismic events are the structural qualities of the bridge decks themselves, rather than the attributes of the underlying soil.

4. Conclusions

Comparative investigations have been conducted to analyse the influence of two distinct soil types, specifically medium-dense sandy soil and stiff clayey soil, on the vulnerability of key components of a bridge. In this work, the generation of seismic fragility curves for the damage states of the bridge piers and deck section was undertaken. The assessment has shown the probability of several damage states for a pier and deck, considering a range of PGA up to 1.5 PGA. Additionally, it is showed that the probability of structural damage occurring during an earthquake is positively correlated with both the PGA and the specific characteristics of the soil. The findings indicate that the deck exhibits lower resilience to seismic events, as it is more likely to sustain minor, moderate, and extensive damage in comparison to the pier. Based on a research paper by Argyroudis and Mitoulis [25], it was found that the reinforced concrete bridge deck component is more susceptible to damage than the pier when subjected to earthquakes and flood scouring hazards. The study investigated the behaviour of reinforced concrete bridge decks under seismic loads and flood scouring conditions. It highlighted that during earthquakes, the lateral forces and ground shaking exert significant stress on the bridge deck, leading to cracking, spalling, and potential failure. The horizontal nature of the bridge deck makes it more vulnerable to these dynamic forces compared to the vertical pier structure. The medium dense sand also exhibited more pronounced damages than that of the clayey soil. The present investigation solely examined the impairment inflicted upon the pivotal elements of the bridge, namely the pier and deck, as well as the two distinct soil types. Phaiand Amin [34] states that soil with poor geotechnical qualities will have a significant impact on the structure constructed on top of it. Consequently, the soil must either be substituted with more robust materials or be stabilised [35]. Soil stabilisation is crucial in construction to guarantee the stability, strength, and stiffness of the soil for any building or structure to be erected [36]. The future study may include the bridge bearings, diaphragm abutments, expansion joints, and stratified soil with diverse properties and the possibility to enhance the scope of analysis to encompass additional potential failure factors, including natural hazards like flood induced-scour and tsunami.

Acknowledgement
This research was funded by a grant from Ministry of Higher Education of Malaysia (FRGS Grant: R0149 - FRGS/1/2022/TK06/UPNM/02/3).

References
[1] Lenggana, Bhre Wangsa, Fitrian Imaduddin, Endra Dwi Purnomo, Dewi Utami, and Saiful Amri Mazlan. "Performance prediction of a novel modular magnetorheological damper for seismic building." *Journal of Advanced Research in Fluid Mechanics and Thermal Sciences* 58, no. 2 (2019): 275-286.
[2] Shuib, Mustaffa Kamal, Mohammad Abdul Manap, Felix Tongkul, Ismail Bin Abd Rahim, Tajul Anuar Jamaludin, Noraini Surip, Rabieahtul Abu Bakar, Mohd Rozaidi Che Abas, Roziah Che Musa, and Zahid Ahmad. "Active faults in Peninsular Malaysia with emphasis on active geomorphic features of Bukit Tinggi region." *Malaysian Journal of Geoscience* 1, no. 1 (2017): 13-26. https://doi.org/10.26480/mjg.01.2017.13.26
[3] Silva, Vitor, Marco Pagani, John Schneider, and Paul Henshaw. "Assessing seismic hazard and risk globally for an earthquake resilient World." *GAR19 Contributing Paper, UNDDR* (2019).

[4] Noh, Muhammad Ramzanee Mohd, Shuib Rambat, Ida Sharmiza Binti Abd Halim, and Fauzan Ahmad. "Seismic risk assessment in Malaysia: A review." *Journal of Advanced Research in Applied Sciences and Engineering Technology* 25, no. 1 (2021): 69-79. https://doi.org/10.37934/araset.25.1.6979
[5] Felix Tongkul, Phd. *Earthquake Science in Malaysia: Status, Challenges and Way Forward*. Universiti Malaysia Sabah Press, 2020.
[6] Rosli, Masli Irwan, Khamarrul Azahari Razak, Faizah Che Ros, and Sumiaty Ambran. "Debris Flow Risk Reduction in Malaysia: From Science-Policy to Multi-Stakeholder Actions." *Journal of Advanced Research in Applied Sciences and Engineering Technology* 24, no. 1 (2021): 18-27. https://doi.org/10.37934/araset.24.1.1827
[7] Tongkul, Felix. "The 2015 Ranau earthquake: Cause and impact." *Sabah Society Journal* 32 (2016): 1-28.
[8] Lei, Xiaoming, Limin Sun, Ye Xia, and Tiantao He. "Vibration-based seismic damage states evaluation for regional concrete beam bridges using random forest method." *Sustainability* 12, no. 12 (2020): 5106. https://doi.org/10.3390/su12125106
[9] Center, JBE. "Damage to Highway Bridges Caused by the 2011 Tohoku-Oki Earthquake." (2011).
[10] Nwe, Zin Zin, Nan Pawt Sai Awar, Aye Mya Cho, Kyaw Moe Aung, Maki Koyama, and Junji Kiyono. "Development of damage patterns and fragility curves in brick-nogging buildings from the thabeikkyin earthquake, Myanmar, 2012." *Journal of Earthquake Engineering* 22, no. 7 (2018): 1169-1187. https://doi.org/10.1080/13632469.2016.1277439
[11] Lin, Chu-Chieh Jay, Hsiao-Hui Hung, Kuang-Yen Liu, and Juin-Fu Chai. "Reconnaissance observation on bridge damage caused by the 2008 Wenchuan (China) earthquake." *Earthquake spectra* 26, no. 4 (2010): 1057-1083. https://doi.org/10.1193/1.3479947
[12] Yang, Ming, Ruey-Juin Rau, Jyh-Yih Yu, and Ting-To Yu. "Geodetically observed surface displacements of the 1999 Chi-Chi, Taiwan, earthquake." *Earth, planets and space* 52, no. 6 (2000): 403-413. https://doi.org/10.1186/BF03352252
[13] Rossetto, Tiziana, and Amr Elnashai. "A new analytical procedure for the derivation of displacement-based vulnerability curves for populations of RC structures." *Engineering structures* 27, no. 3 (2005): 397-409. https://doi.org/10.1016/j.engstruct.2004.11.002
[14] Kim, Kyeongjin, and Jaeha Lee. "Fragility of bridge columns under vehicle impact using risk analysis." *Advances in Civil Engineering* 2020, no. 1 (2020): 7193910. https://doi.org/10.1155/2020/7193910
[15] Zhang, Chao, Jianbin Lu, Zhengan Zhou, Xueyuan Yan, Li Xu, and Jinjun Lin. "Lateral Seismic Fragility Assessment of Cable-Stayed Bridge with Diamond-Shaped Concrete Pylons." *Shock and Vibration* 2021, no. 1 (2021): 2847603. https://doi.org/10.1155/2021/2847603
[16] Kim, Hyunjun, Sung-Han Sim, Jaebeom Lee, Young-Joo Lee, and Jin-Man Kim. "Flood fragility analysis for bridges with multiple failure modes." *Advances in Mechanical Engineering* 9, no. 3 (2017): 1687814017696415. https://doi.org/10.1177/1687814017696415
[17] Su, Jie, Zhenghua Zhou, You Zhou, Xiaojun Li, Qing Dong, Yafei Wang, Yuping Li, and Liu Chen. "The characteristics of seismic response on hard interlayer sites." *Advances in Civil Engineering* 2020, no. 1 (2020): 1425969. https://doi.org/10.1155/2020/1425969
[18] Argyroudis, Sotirios, Stergios Mitoulis, Mike G. Winter, and Amir M. Kaynia. "Fragility of critical transportation infrastructure systems subjected to geo-hazards." In *Proceedings 16th European Conference on Earthquake Engineering*. European Conference on Earthquake Engineering, 2018. https://doi.org/10.1061/9780784481479.018
[19] Lin, Xiangfeng, Jisheng Zhang, Dawei Guan, Jinhai Zheng, Hailong Wang, and Bo Liu. "Scour processes around a mono-pile foundation under bi-directional flow considering effects from a rotating turbine." *Ocean Engineering* 269 (2023): 113401. https://doi.org/10.1016/j.oceaneng.2022.113401
[20] FEMA 356, FEDERAL EMERGENCY. "Prestandard and commentary for the seismic rehabilitation of buildings." *Federal Emergency Management Agency: Washington, DC, USA* (2000).
[21] Haselton, C. B., A. S. Whittaker, Ayse Hortacsu, J. W. Baker, Jonathan Bray, and D. N. Grant. "Selecting and scaling earthquake ground motions for performing response-history analyses." In *Proceedings of the 15th world conference on earthquake engineering*, pp. 4207-4217. Oakland, CA, USA: Earthquake Engineering Research Institute, 2012.
[22] Mehani, Youcef, Abderrahmane Kibboua, Benazouz Chikh, and Mustapha Remki. "Seismic vulnerability of an existing strategic RC building using non linear static and dynamic analyses." *Građevinar* 72, no. 07. (2020): 617-626. https://doi.org/10.14256/JCE.2122.2017
[23] Argyroudis, Sotirios, Stergios Mitoulis, Mike G. Winter, and Amir M. Kaynia. "Fragility of critical transportation infrastructure systems subjected to geo-hazards." In *Proceedings 16th European Conference on Earthquake Engineering*. European Conference on Earthquake Engineering, 2018. https://doi.org/10.1061/9780784481479.018

[24] Mackie, K. R., and B. Stojadinović. "Performance-based seismic bridge design for damage and loss limit states." *Earthquake engineering & structural dynamics* 36, no. 13 (2007): 1953-1971. https://doi.org/10.1002/eqe.699
[25] Argyroudis, Sotirios A., and Stergios Aristoteles Mitoulis. "Vulnerability of bridges to individual and multiple hazards-floods and earthquakes." *Reliability engineering & system safety* 210 (2021): 107564. https://doi.org/10.1016/j.ress.2021.107564
[26] McKenna, Gregory, Sotirios A. Argyroudis, Mike G. Winter, and Stergios A. Mitoulis. "Multiple hazard fragility analysis for granular highway embankments: Moisture ingress and scour." *Transportation Geotechnics* 26 (2021): 100431. https://doi.org/10.1016/j.trgeo.2020.100431
[27] Yuan, Leung Fo Vincent, Sotirios A. Argyroudis, Enrico Tubaldi, Maria Pregnolato, and Stergios A. Mitoulis. "Fragility of bridges exposed to multiple hazards and impact on transport network resilience." In *Proceedings of the 2019 Society for Earthquake and Civil Engineering Dynamics conference (SECED 2019)*. Society for Earthquake and Civil Engineering Dynamics (SECED), 2019.
[28] Jain, Ankit, Robin Davis, and CG Nanda Kumar. "Seismic fragility analysis of bridge pier." In *IOP Conference Series: Materials Science and Engineering*, vol. 936, no. 1, p. 012014. IOP Publishing, 2020. https://doi.org/10.1088/1757-899X/936/1/012014
[29] Kim, Sang-Hoon, and Masanobu Shinozuka. "Development of fragility curves of bridges retrofitted by column jacketing." *Probabilistic Engineering Mechanics* 19, no. 1-2 (2004): 105-112. https://doi.org/10.1016/j.probengmech.2003.11.009
[30] Argyroudis, Sotiris, and Amir M. Kaynia. "Analytical seismic fragility functions for highway and railway embankments and cuts." *Earthquake Engineering & Structural Dynamics* 44, no. 11 (2015): 1863-1879. https://doi.org/10.1002/eqe.2563
[31] Annad, Mohamed, Nadjib Hemaidi Zourgui, Abdelouahab Lefkir, Abderrahmane Kibboua, and Oussama Annad. "Scour-dependent seismic fragility curves considering soil-structure interaction and fuzzy damage clustering: A case study of an Algerian RC Bridge with shallow foundations." *Ocean Engineering* 275 (2023): 114157. https://doi.org/10.1016/j.oceaneng.2023.114157
[32] Tsionis, Georgios, and Michael N. Fardis. "Fragility functions of road and railway bridges." In *SYNER-G: Typology Definition and Fragility Functions for Physical Elements at Seismic Risk: Buildings, Lifelines, Transportation Networks and Critical Facilities*, pp. 259-297. Dordrecht: Springer Netherlands, 2013. https://doi.org/10.1007/978-94-007-7872-6_9
[33] Aydinoglu, M. N. "An improved pushover procedure for engineering practice: Incremental Response Spectrum Analysis (IRSA)." In *Proceedings of the Workshop "Performance-based seismic design. Concepts and implementation*, no. 2004/05, pp. 345-356. PEER Report, 2004.
[34] Phai, Hengchhorn, and Amin Eisazadeh. "Geotechnical properties of rice husk ash-lime-stabilised Bangkok clay." *Journal of Engineering Science and Technology* 15, no. 1 (2020): 198-215.
[35] Latib, Farah Wahida Mohd, Anuar Kasa, and Mohd Fairuz Bachok. "Geotechnical Properties on Residual Soil of Sedimentary Rock." *Journal of Advanced Research in Applied Sciences and Engineering Technology* 30, no. 3 (2023): 182-191. https://doi.org/10.37934/araset.30.3.182191
[36] Nor, Ahmad Hakimi Mat, Saiful Azhar Ahmad Tajudin, Faizal Pakir, Mohd Erwan Sanik, and Salman Salim. "Influence of Biomass Silica Stabilizer on Unconfined Compression Strength of Sodium Silicate Stabilized Soft Clay Soils." *Journal of Advanced Research in Applied Sciences and Engineering Technology* 28, no. 1 (2022): 97-105. https://doi.org/10.37934/araset.28.1.97105